Journal of Power Sources 255 (2014) 387–393

Contents lists available at ScienceDirect

Journal of Power Sources

journal homepage: www.elsevier.com/locate/jpowsour

Short communication

Enhanced utilization and durability of Pt nanoparticles supported on sulfonated carbon nanotubes

Lin Guo, Siguo Chen*, Zidong Wei*

The State Key Laboratory of Power Transmission Equipment & System Security and New Technology, College of Chemistry and Chemical Engineering, Chongqing University, Chongqing 400044, China

HIGHLIGHTS

- The sulfonic group has been successfully linked onto the CNTs surface.
- The Pt/SO_3H–Ar–CNTs exhibits high Pt utilization and low Nafion dependence.
- The durability of the Pt/SO_3H–Ar–CNTs has been greatly improved.

ARTICLE INFO

Article history:
Received 6 October 2013
Received in revised form
5 January 2014
Accepted 8 January 2014
Available online 15 January 2014

Keywords:
Proton exchange membrane fuel cell
Sulfonated carbon nanotubes
High platinum utilization
Improved catalyst durability

ABSTRACT

We have synthesized a hybrid catalyst with the high Pt utilization and durability, in which the Pt nanoparticles are deposited on the sulfonated carbon nanotubes (SO_3H–Ar–CNTs) with conducting proton and electron. Electrochemical performance of the catalyst (Pt/SO_3H–Ar–CNTs) is evaluated by the cyclic voltammograms, linear sweep voltammetry and fuel cell tests, respectively. The experimental results demonstrate that the Pt/SO_3H–Ar–CNTs catalyst exhibits good oxygen reduction reaction activity, enhanced durability and excellent Pt utilization compared with the Pt/COOH–CNTs catalyst. The improved performance of Pt/SO_3H–Ar–CNTs catalyst is ascribed to the introduction of the sulfonic acid group onto the CNTs surface by the covalent modification method, which ensures Pt NPs locate in triple-phase zones to increase Pt utilization and reduces the corrosion of the SO_3H–Ar–CNTs.

1. Introduction

Proton exchange membrane fuel cells (PEMFCs) have been attracted considerable attention as promising energy conversion devices for various applications in portable electronics, automotive engines and stationary generation systems [1,2]. So far, Pt-based catalysts remain the most effective electrocatalysts for the commercial fuel cells [3–5]. However, the high cost, limited supply, and poor durability of Pt have hindered the widespread application of PEMFCs [5,6]. It has been estimated that the Pt catalyst used in the electrodes possesses about 40% of the total cost of fuel cells [7]. Therefore, decreasing the cost of PEMFCs via the increase of the utilization efficiency and the durability of Pt has been one of the major concerns. Because catalysis at the electrode of PEMFCs is an interface phenomenon, electrode reactions can occur only at confined spatial sites called triple-phase zones where the Pt nanoparticles (NPs) have simultaneous access to the reactants, the electron transport medium, and the proton transport medium. Conventionally, incorporating a certain amount of Nafion into the electrode is the most effective strategy to obtain the triple-phase zones [8]. However, Nafion for protons transport tends to wrap or isolate Pt NPs on the electrode, leading to the interruption of proton and electron channels, the increase of gas transport resistance and finally to the low Pt utilization [9]. Hence, numerous researches have focused on optimizing the composition and structure of the electrodes to increase the exposure of Pt NPs into the triple-phase zones on the electrode [8,10–13]. Sun et al. [14] synthesized one Pt-Nafion/C catalyst by a modified ion-exchange method, in which $[Pt(NH_3)_2]^{2+}$ cations were ion-exchanged onto the oxidatively-treated carbon coated by Nafion and then reduced by H_2 to fabricate the triple-phase zones, resulting in an improved Pt utilization in fuel cells. Watanabe et al. [15] studied that Nafion was penetrated into the primary pores of Pt/C catalyst agglomerates by autoclave treatment. They found that Nafion was distributed more uniformly in the primary pores of Pt/C catalyst agglomerates, which obtained a better polarization property by the higher Pt catalyst

* Corresponding authors. Tel.: +86 23 65105161; fax: +86 23 65102531.
E-mail addresses: csg810519@126.com (S. Chen), zdwei@cqu.edu.cn (Z. Wei).

0378-7753/$ – see front matter © 2014 Elsevier B.V. All rights reserved.
http://dx.doi.org/10.1016/j.jpowsour.2014.01.040

utilization. Wei et al. [16] reported an alternative ion-exchange/electrodeposition (AIEE) method, in which carbon black was first bonded with polytetrafluoroethylene and then coated with Nafion. It has been found that the Pt utilization of AIEE electrode, reflected by fuel cell output power density, was 2.2 times higher than that of conventional electrodes. Although these strategies have been proposed to increase the Pt utilization, the processes of preparing the three-phase zones are too complex and seriously dependent on the loading and distribution of Nafion. More importantly, the proton and electron transports were still severally achieved by Nafion and carbon supports in the three-phase zones, respectively, which cannot ensure each Pt NPs locate into the three-phase zones and then be used as activity site. Thus, developing a kind of material conducting both electron and proton to make each Pt NPs in the three-phase zones is highly desirable.

Herein, we present a novel bifunctional support with the ability to conduct proton as well as electron prepared by using the covalent modification method [17] to link the benzene sulfonic acid groups (−Ar−SO_3H) onto the surface of carbon nanotubes (CNTs), called as sulfonated CNTs (SO_3H−Ar−CNTs). The SO_3H−Ar−CNTs have abundant −SO_3H groups on the CNTs surface through the benzene rings, which can ensure the excellent electrical conductivity between the Pt NPs and CNTs in the Pt/SO_3H−Ar−CNTs catalyst. More importantly, the −SO_3H groups on the surface of CNTs not only serve as the anchor centers for achieving high Pt dispersion, but also act as the proton transport centers of Pt NPs, which realize that proton and electron transport channels can simultaneously appear on the Pt NPs surface and then allow each Pt NPs supported on the SO_3H−Ar−CNTs to locate into the triple-phase zones on the electrode, greatly enhancing the utilization of Pt NPs and reducing the amount of Nafion. Moreover, the SO_3H−Ar−CNTs synthesized by the covalent modification could hardly cause the structural damage of CNTs compared with the COOH−CNTs prepared by the conventional acid oxidation method, which is conducive to decreasing the corrosion of the SO_3H−Ar−CNTs and improving the durability of Pt/SO_3H−Ar−CNTs.

2. Experimental

2.1. Preparation of catalysts

The pristine CNTs (Shenzhen Nanotech Port Co. Ltd.) was first purified by being immersed in concentrated HCl solution for 5 days and then refluxed for 5 h, followed by diluting, filtering, washing and vacuum drying at 80 °C overnight. The carboxylation of the purified CNTs was then carried out in H_2SO_4/H_2O_2 mixture solution (4:1 by volume) for 3 h, followed by diluting, filtering, washing and vacuum drying at 80 °C overnight. The product was called as COOH−CNTs. The SO_3H−Ar−CNTs sample was performed using a covalent modification method [17], in which isoamyl nitrite solution was slowly added to the mixture of purified CNTs and sodium *p*-aminobenzenesulfonate via syringe in a round bottom flask. The reaction mixture was vigorously stirred and heated at 60 °C for an hour, followed by filtering and washing with DMF and diethyl ether. The product was collected and dried under vacuum at 50 °C for overnight.

Pt NPs supported on COOH−CNTs and SO_3H−Ar−CNTs were synthesized by the ethylene glycol (EG) reduction method. Briefly, 80 mg of CNTs support, 60 mg of sodium citrate and 1 mL of H_2PtCl_6 solution (20 mg mL^{-1} Pt) were mixed with 35 mL of EG, followed by stirring for 30 min and adjusting the pH to 11 using 1 M NaOH in EG solution. The mixture was then placed into a Teflon-lined autoclave and conditioned at 160 °C for 6 h, followed by filtering, washing and vacuum drying at 80 °C. The Pt loading of all the catalysts was controlled at 20 wt.%. The prepared Pt catalyst supported on COOH−CNTs, and SO_3H−Ar−CNTs was denoted by Pt/COOH−CNTs and Pt/SO_3H−Ar−CNTs, respectively.

2.2. Electrochemical measurements

All electrochemical experiments were performed in a standard three-electrode cell at room temperature. The half cell consisted of a glassy carbon working electrode (GC electrode, 5 mm in diameter), an Ag/AgCl (saturated KCl) reference electrode, and a platinum foil counter electrode. All potentials in this study, however, are given relative to the reversible hydrogen electrode (RHE). The working electrodes were prepared by applying catalyst inks onto GC disk. In brief, the electrocatalyst was dispersed in ethanol and ultrasonicated for 10 min to form a uniform catalyst ink. A total of 10 μL of well-dispersed catalyst ink was applied onto a prepolished GC disk. After drying at room temperature, a drop of 0.5 wt.% Nafion solution was applied onto the surface of the catalyst layer to form a thin protective film. The prepared electrodes were dried at room temperature before electrochemical tests.

The accelerated durability tests (ADT) were performed at potentials between 0 and 1.2 V at a scan rate of 50 mV s^{-1} in N_2-purged 0.1 M $HClO_4$ at room temperature. The CV curves were recorded every 50 cycles to calculate the electrochemical surface area (ECSA) of Pt in the catalysts using the following equation [4,18,19]:

$$\mathrm{ECSA} = \frac{Q_H}{0.21\ \mathrm{mC\ cm^{-2}} \times [\mathrm{Pt}]}$$

where Q_H (mC) is the charge due to the hydrogen adsorption/desorption in the hydrogen region (0.05−0.40 V) of the CVs, [Pt] is the loading of Pt on the working electrode, and 0.21 mC cm^{-2} is the electrical charge required to oxidize a monolayer of hydrogen on Pt, corresponding to a surface density of 1.3×10^{15} Pt atoms per cm^2, which is generally accepted for polycrystalline Pt electrodes.

All of the electrodes were pretreated by cycling the potential between 0.05 and 1.1 V at a sweep rate of 50 mV s^{-1} for 50 cycles to remove any surface contamination prior to ORR activity test. The ORR polarization curves were conducted in O_2-saturated 0.1 M $HClO_4$ solution at a scan rate of 10 mV s^{-1}. The rotation speed was controlled at 1600 rpm.

2.3. Preparation and performance measurement of membrane electrode assembly (MEA)

Catalyst inks for cathode were prepared by mixing the Pt/SO_3H−Ar−CNTs catalysts or the Pt/COOH−CNTs catalyst, 5 wt.% Nafion solution (DuPont), and anhydrous alcohol. Different percentages of Nafion ranging from 0 to 50 wt.% (weight percentage in deposited solid fraction) were added to the suspension. Catalyst inks for anode were prepared by mixing Pt/C catalyst (Johnson-Matthey In. UK), 5 wt.% Nafion solution, and anhydrous alcohol. The weight ratio of catalyst loading to solid Nafion was maintained at 3:1 on the anodic side. All of the well dispersed suspensions were obtained by immersing the catalyst inks in an ultrasonic bath during at least 15 min. The suspensions were pipetted onto the carbon paper and finally heated at 80 °C for 10 min. The MEA was prepared by hot-pressing the cathode, Nafion 112 membrane (DuPont), and the anode at 137 °C and 5 MPa for 2 min. The Pt loading was controlled at 0.3 mg cm^{-2} on the anodic side and 0.1 mg cm^{-2} on the cathodic side. The effective area of the electrode was 5 cm^{-2}. The Nafion 112 membrane was pretreated with 3 vol.% H_2O_2 and 0.5 M H_2SO_4 for 1 h to remove impurities. The membrane was then washed several times with hot deionized water.

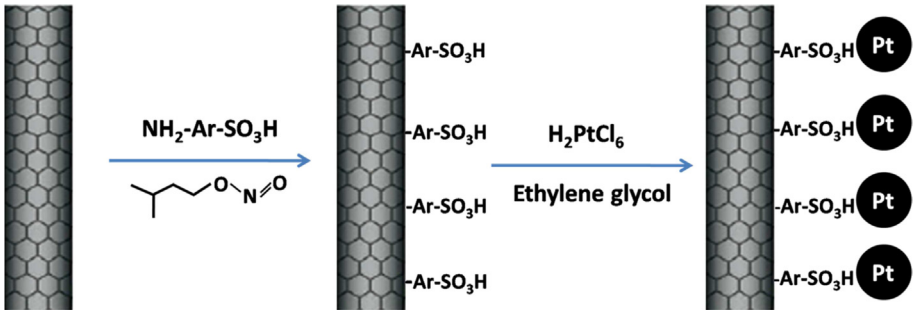

Scheme 1. Schematic illustration of the synthesis of the Pt/SO_3H–Ar–CNTs catalyst.

The polarization curves of MEA were measured with the Fuel Cell Test Station (Fuel Cell Technologies, Inc.). The electrochemical polarization behavior was obtained at 80 °C. The hydrogen and oxygen were supplied to the anode and cathode at flow rates of 350 and 500 mL min^{-1}, respectively. The back pressure for the anode and cathode were zero and 90 kPa, respectively. The gas humidification temperatures were 5 °C lower than the cell temperature for hydrogen and oxygen, respectively.

2.4. FTIR test

The FTIR spectra were recorded on a Nicolet 550II FTIR spectrometer.

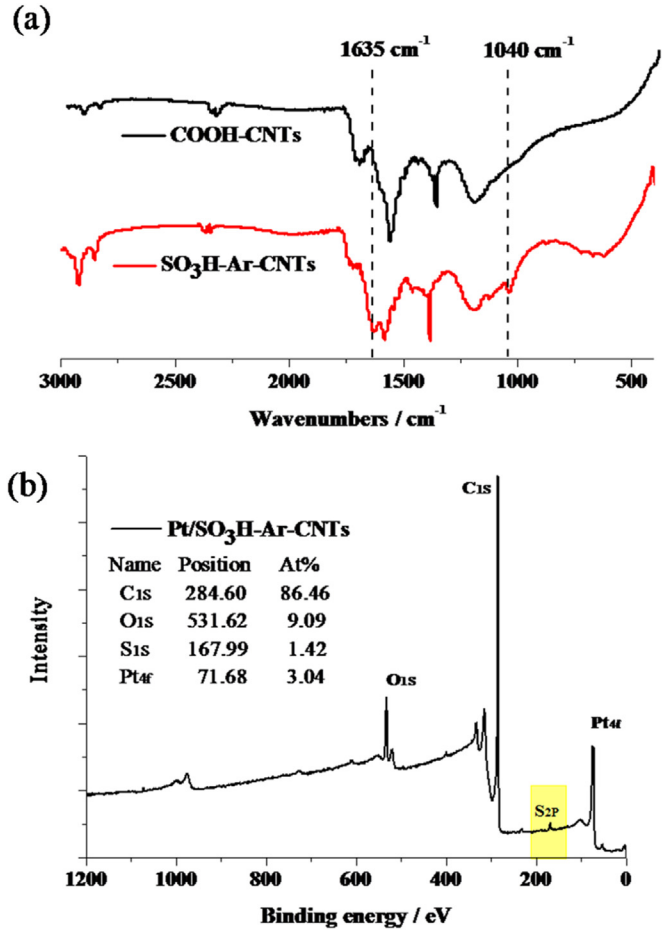

Fig. 1. (a) FTIR spectra of COOH–CNTs and SO_3H–Ar–CNTs, (b) XPS spectra of Pt/SO_3H–Ar–CNTs catalyst.

2.5. TEM test

Transmission electron microscopy (TEM) was carried out on a Zeiss LIBRA 200 FETEM instrument operating at 200 kV.

2.6. XPS analysis

XPS spectra were acquired by using a PE PHI-5400 spectrometer equipped with a monochromatic Al X-ray source (Al KR, 1.4866 keV).

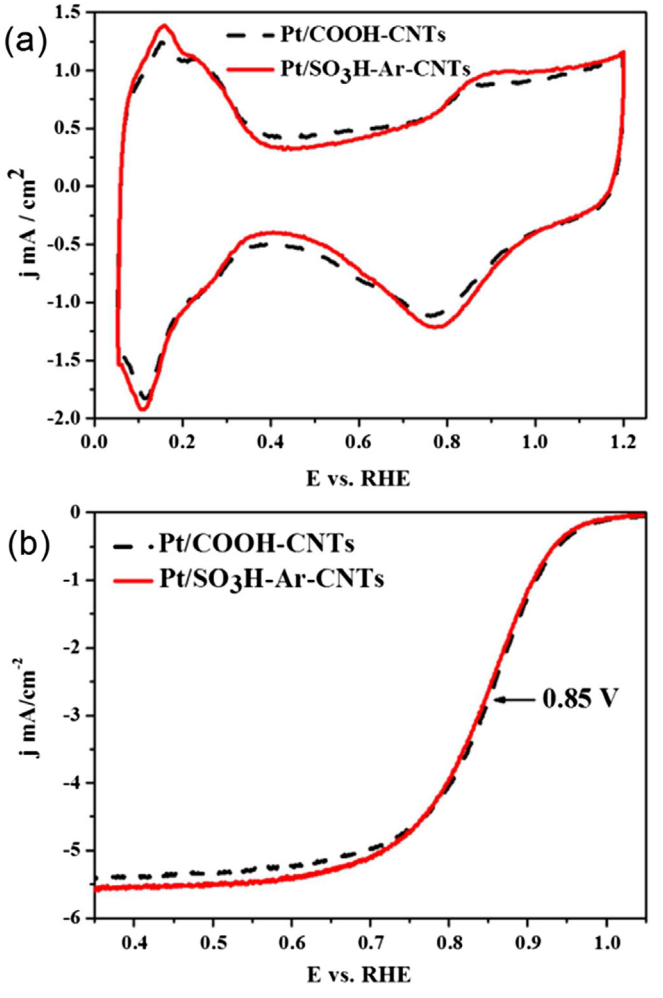

Fig. 2. (a) CV curves of electrodes made with Pt/COOH–CNTs and Pt/SO_3H–Ar–CNTs in N_2-purged 0.1 M $HClO_4$ solution at a scan rate of 50 mV s^{-1}. (b) ORR curves of electrodes made from Pt/COOH–CNTs and Pt/SO_3H–Ar–CNTs in O_2-saturated 0.1 M $HClO_4$ solution at room temperature (1600 rpm, scan rate 10 mV s^{-1}).

3. Results and discussion

The fabrication process for the Pt/SO_3H–Ar–CNTs catalyst is demonstrated in Scheme 1. First, the SO_3H–Ar–CNTs was prepared via covalent modification method to introduce –Ar–SO_3H groups onto the CNTs surface. Afterward, Pt NPs were deposited onto the SO_3H–Ar–CNTs surface to form the Pt/SO_3H–Ar–CNTs catalyst by EG reduction method. The prepared SO_3H–Ar–CNTs were first characterized by FTIR spectroscopy. As shown in Fig. 1a, there are two new peaks at 1635 cm^{-1} and 1040 cm^{-1}, which are attributed

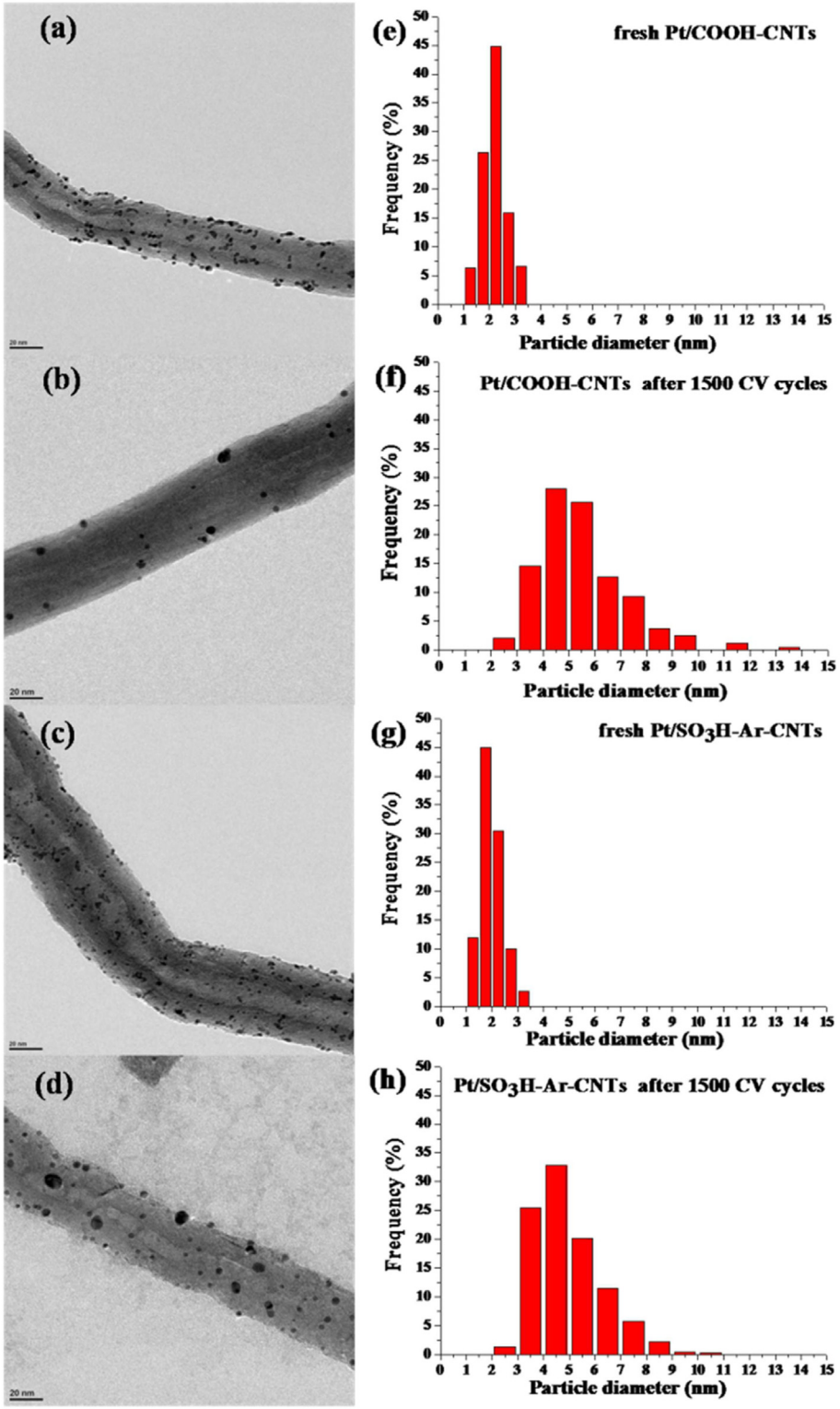

Fig. 3. TEM images (left) and size distributions (right) of nanoparticles of nanohybrids. (a), (e) fresh Pt/COOH–CNTs; (b), (f) aged Pt/COOH–CNTs after 1500 CV cycles; (c), (g) fresh Pt/SO_3H–Ar–CNTs; (d), (h) aged Pt/SO_3H–Ar–CNTs after 1500 CV cycles.

to the vibration bands of the aromatic C–H and the $-SO_3H$ groups, respectively [20,21]. These representative peaks successfully indicate introduction of the $-SO_3H$ groups on CNTs. X-ray photoelectron spectroscopy (XPS) was carried out to determine the chemical composition of the prepared Pt/SO_3H–Ar–CNTs catalysts. Fig. 1b shows the atomic percentage of all the elements of Pt/SO_3H–Ar–CNTs catalyst, in which the percentage of S element is estimated to be 1.42%.

Before discussing the beneficial effect of the $-SO_3H$ group on fuel cell performance, the electrochemical and electrocatalytic behaviors of the Pt/COOH–CNTs and Pt/SO_3H–Ar–CNTs catalysts were evaluated. Typical cyclic voltammograms (CV) of the Pt/COOH–CNTs and Pt/SO_3H–Ar–CNTs catalysts recorded in N_2-puraged 0.1 M $HClO_4$ are shown in Fig. 2a. The electrochemical surface areas (ECSA) of the Pt/COOH–CNTs and Pt/SO_3H–Ar–CNTs catalysts were estimated to be 57.2 $m^2\ g^{-1}$ and 59.0 $m^2\ g^{-1}$, respectively. The similar ECSA can be attributed to the small size and good dispersion of Pt NPs on the COOH–CNTs and SO_3H–Ar–CNTs (see the TEM images in Fig. 3a, c), confirming that the SO_3H–Ar–CNTs is suitable to anchor Pt NPs and also to be serviced as supports for electrocatalyst. Subsequently, the linear sweep voltammetry (LSV) measurements were recorded on a rotating disk electrode (RDE) to investigate the oxygen reduction reaction (ORR) performance for the Pt/COOH–CNTs and Pt/SO_3H–Ar–CNTs catalysts in O_2-saturated 0.1 M $HClO_4$ at a scan rate of 10 mV s^{-1} and a rotation rate of 1600 rpm. As can be seen in Fig. 2b, the Pt/SO_3H–Ar–CNTs catalyst exhibits the similar half-wave potentials (~0.85 V) and activity with respect to the Pt/COOH-CNTs catalyst, confirming that the $-SO_3H$ groups have no effect on the oxygen reduction activity of the catalyst.

Different from that in half cell tests, electrochemical reactions can only continuously occur at triple-phase zones in single cell test. In order to evaluate the performance of the Pt/SO_3H–Ar–CNTs catalyst in the enhancement of Pt utilization, the single cell tests were further examined at 80 °C with pure hydrogen and oxygen at the anode and cathode, respectively. The Pt loading at the cathode was 0.1 mg cm^{-2}, whereas the Pt loading at anode was deliberately high (0.3 mg cm^{-2}) to avoid impact on the overall fuel cell performance. The ECSA of the Pt/COOH–CNTs and Pt/SO_3H–Ar–CNTs catalyst in the MEA, as shown in Fig. 4a, were also examined using LSV measurements. As expected, the Pt/SO_3H–Ar–CNTs catalyst (~30 $m^2\ g_{Pt}^{-1}$) shows the bigger ECSA than the Pt/COOH–CNTs catalyst (~22 $m^2\ g_{Pt}^{-1}$), suggesting that the Pt/SO_3H–Ar–CNTs catalyst could possess a higher Pt utilization than the Pt/COOH–CNTs catalyst in the MEA. Fig. 4b shows the polarization curves of the Pt/COOH–CNTs and Pt/SO_3H–Ar–CNTs catalysts for the single cells without Nafion in the cathode catalyst layer. The Pt/COOH–CNTs and Pt/SO_3H–Ar–CNTs catalysts without Nafion exhibit the peak power densities of 398 and 714 mW cm^{-2}, respectively. It is worth noting that the peak power density of 398 mW cm^{-2} for the Pt/COOH–CNTs catalyst should be primarily ascribed to the combination between Nafion membrane and the catalysts on the surface of the catalyst layer by the hot-pressing process, which supplies a few paths of proton transport to the Pt NPs near the Nafion membrane, but have little effect on the Pt NPs located in the depth of the catalyst layer far away from the Nafion membrane. Correspondingly, the peak power density of the Pt/SO_3H–Ar–CNTs catalyst is about 1.8 times higher than that of the Pt/COOH–CNTs catalyst. Considering that the preparation process of the electrodes, the dispersion and the electrochemical activity of Pt NPs are similar for Pt/SO_3H–Ar–CNTs and Pt/COOH–CNTs catalysts, the highly improved Pt utilization for the Pt/SO_3H–Ar–CNTs catalyst should not simply be ascribed to the hot-pressing process, but the defined deposition of Pt NPs on the SO_3H–Ar–CNTs, which provides more the paths of proton and electron transport for the Pt NPs and makes a large amount of the Pt NPs locate in triple-phase zones without the presence of Nafion.

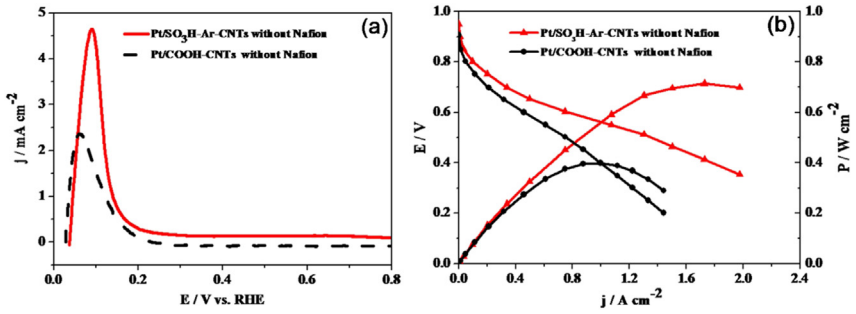

Fig. 4. (a) LSV curves of the cathodes made from Pt/COOH–CNTs and Pt/SO_3H–Ar–CNTs in MEA at 80 °C; cathodes are protected by high purity nitrogen; anodes are fed with hydrogen at 50 mL min^{-1}; the scan rate is 50 mV s^{-1}. (b) Performance curves of the single cells with Pt/COOH–CNTs and Pt/SO_3H–Ar–CNTs as the cathode catalysts without Nafion and Pt/C as the anode catalyst with 25 wt.% Nafion.

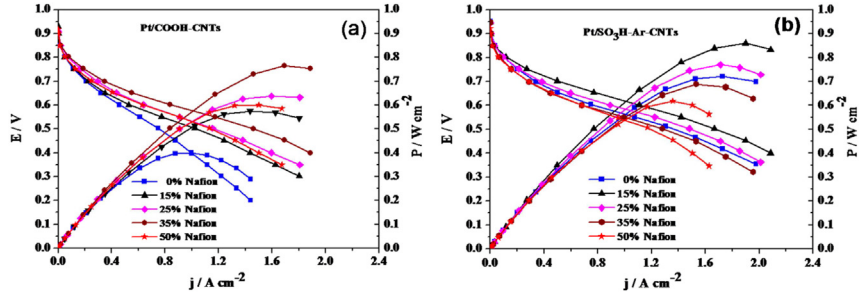

Fig. 5. Performance curves of the single cells with (a) Pt/COOH–CNTs and (b) Pt/SO_3H–Ar–CNTs as the cathode catalysts with different Nafion loadings and Pt/C as the anode catalysts with 25 wt.% Nafion.

To better understand the potency and capability of the $-SO_3H$ groups on the Pt utilization in the single cell, the cell performance for cathode electrodes made using Pt/COOH–CNTs and Pt/SO_3H–Ar–CNTs catalyst with different Nafion loadings were evaluated in the single cell. Fig. 5 shows the performance of a series of Pt/COOH–CNTs and Pt/SO_3H–Ar–CNTs catalysts with various Nafion loadings in the range of 0–50 wt.%. It can be seen in Fig. 5a that the performance of the Pt/COOH–CNTs catalyst has been obviously improved with the increase of Nafion loading from 0 to 35 wt.%, but further increasing the Nafion loading to 50 wt.% resulted in a sharp decline in performance, conforming that Nafion plays a vital role for improving the Pt utilization of the Pt/COOH–CNTs catalyst and too low or too much Nafion will cause the evident decline in the performance. Therefore, the best performance of the Pt/COOH–CNTs catalyst in the single cell has been attained at the optimum 35 wt.% Nafion. These results indicate that the cell performance of the Pt/COOH–CNTs catalyst in cathode layer strongly depends on the high loading and distribution of Nafion. In contrast, the Pt/SO_3H–Ar–CNTs catalyst in the single cell represents less dependence on the Nafion relative to the Pt/COOH–CNTs catalyst. As shown in Fig. 5b, the Pt/SO_3H–Ar–CNTs catalyst in the single cell exhibits the best peak power density of 860 mW cm^{-2} with only 15 wt.% Nafion, which is obviously higher than that (766 mW cm^{-2}) of the Pt/COOH–CNTs catalyst with as high as 35 wt.% Nafion, conforming that the Pt/SO_3H–Ar–CNTs catalyst effectively reduces the use of Nafion and also significantly enhances the Pt utilization owing to the excellent electron and proton transport abilities of the SO_3H–Ar–CNTs with respect to the COOH–CNTs. In addition, the best performance of the Pt/SO_3H–Ar–CNTs catalyst in single cell with 15 wt.% Nafion demonstrates that Nafion is still needed for the Pt/SO_3H–Ar–CNTs catalyst to facilitate proton transport among the catalyst particles. However, a slight excess of Nafion for the Pt/SO_3H–Ar–CNTs catalyst is more easy to reduce the fuel cell performance compared with the Pt/COOH–CNTs catalyst owing to a large amount of the $-SO_3H$ group linked on the Pt/SO_3H–Ar–CNTs catalyst, which easily causes local accumulation of liquid water to flood the catalyst surface and hinders gas diffusion in the catalyst layer.

Apart from Pt utilization, durability of the catalysts is another obstacle that has hindered the development of PEMFCs. To evaluate the durability of the Pt/COOH–CNTs and Pt/SO_3H–Ar–CNTs catalysts, accelerated durability tests (ADT) were done by applying potential sweeps between 0 and 1.2 V vs. RHE at 50 mV s^{-1} in N_2-puraged 0.1 M $HClO_4$ at room temperature. The Pt ECSA values for the Pt/COOH–CNTs and Pt/SO_3H–Ar–CNTs catalysts after potential cycling were calculated from their respective CVs (Fig. 6b, c), and the normalized ECSA to the highest values was plotted as a function of the cycle numbers (Fig. 6a). After 1500 accelerated cycles, the Pt/SO_3H–Ar–CNTs catalyst only decreased ~26% of its initial ECSA, whereas the Pt/COOH–CNTs catalyst lost ~91% of the initial ECSA. The morphologies of the Pt/COOH–CNTs and Pt/SO_3H–Ar–CNTs catalysts before and after the 1500 cycles were examined by TEM (Fig. 3a–d). The size distribution of the Pt NPs calculated according to Fig. 3a–d is shown in Fig. 3e–h. The size of the Pt NPs in the Pt/COOH-CNTs catalyst increased from 2–4 to 3–14 nm after 1500 accelerated cycles (Fig. 3e, f), indicating that ripening or aggregation of the Pt NPs occurred during the CV cycling. Meanwhile, the TEM images (Fig. 3a, b) show the loss and detachment of Pt NPs from CNTs in Pt/COOH–CNTs catalysts, confirming that the major cause for the Pt ECSA loss of Pt/COOH-CNTs was by the loss of Pt NPs from the CNT support owing to its own corrosion. This assertion can also be verified by the oxidation peak (~0.7 V) of the COOH–CNTs during the CV ADT test as shown in Fig. 6b. This result is consistent with the conclusion by Kim and Wei [22,23] that the aggressive oxidative treatment of graphitized carbon leads to the decay of catalyst performance. Compared with the Pt/COOH–CNTs catalyst, the size of the Pt NPs in the Pt/SO_3H–Ar–CNTs catalyst shows the relatively small increase from 1–3 to 3–11 nm (Fig. 3g, h). In combination with the TEM images (Fig. 3a–d), the result demonstrates that the Pt/SO_3H–Ar–CNTs catalyst is more electrochemically stable than the Pt/COOH–CNTs catalyst. The improved

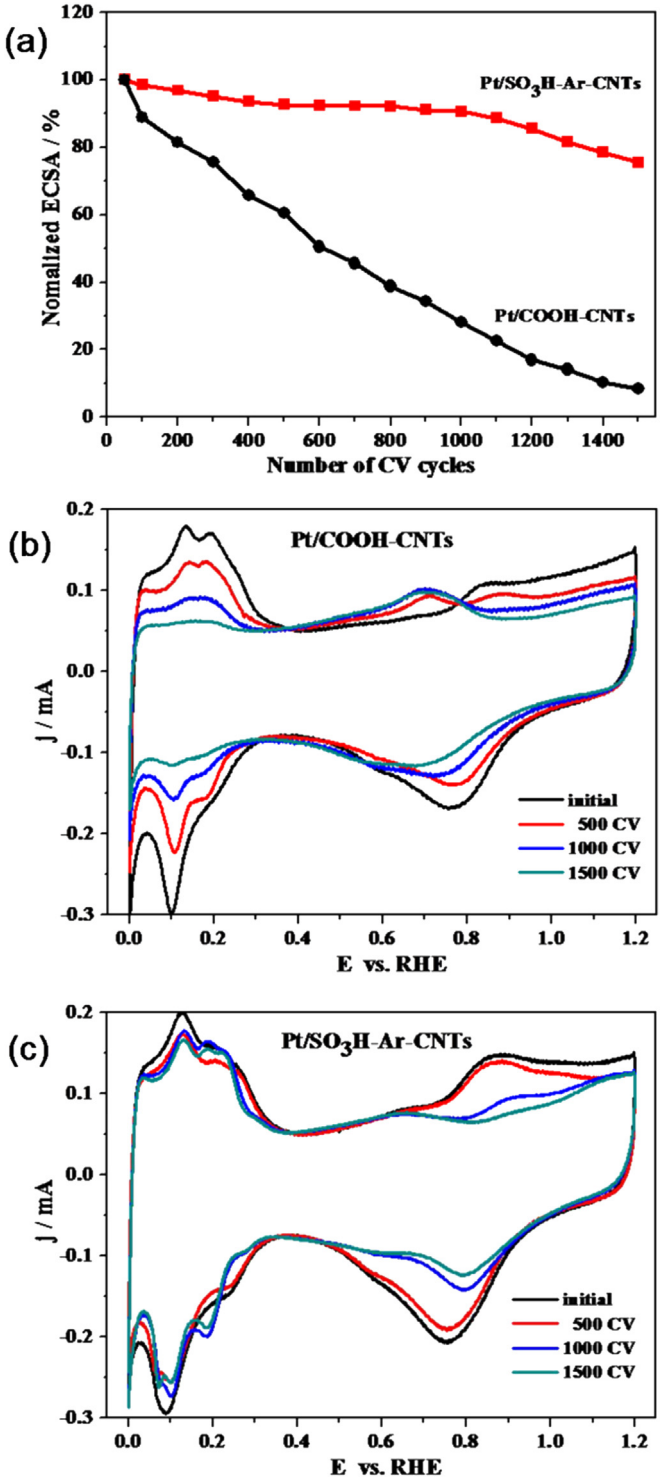

Fig. 6. (a) Normalized Pt ECSA of electrodes made with Pt/COOH–CNTs and Pt/SO_3H–Ar–CNTs in N_2-purged 0.1 M $HClO_4$ at room temperature (0–1.2 V vs. RHE, sweep rate 50 mV s^{-1}). CV curves of electrodes made from (b) Pt/COOH–CNTs and (c) Pt/SO_3H–Ar–CNTs at different CV cycles in N_2-purged 0.1 M $HClO_4$ solution at a scan rate of 50 mV s^{-1}.

durability of the Pt/SO_3H–Ar–CNTs catalyst should be correlated with the covalent modification method, which can effectively avoid the serious damage of CNTs surface compared with the harsh acid oxidation method, and then is helpful for decreasing the SO_3H–Ar–CNTs corrosion to benefit the durability of the Pt/SO_3H–Ar–CNTs catalyst.

4. Conclusion

In summary, we have successfully prepared a Pt/SO_3H–Ar–CNTs catalyst with enhanced Pt utilization and durability via the surface sulfonation of CNTs. Compared with the Pt/COOH–CNTs catalyst, the Pt/SO_3H–Ar–CNTs catalyst has exhibited high Pt utilization and less dependence on the Nafion. The improved performance of the Pt/SO_3H–Ar–CNTs catalyst is due to the $-SO_3H$ groups linked onto the CNTs surface, which integrates proton and electron transport channels into the CNTs to offer more triple-phase zones on Pt NPs surfaces. The covalent modification method effectively reduces the SO_3H–Ar–CNTs corrosion and improves the durability of the Pt/SO_3H–Ar–CNTs catalyst with respect to the Pt/COOH–CNTs catalyst. The present study demonstrates that the Pt/SO_3H–Ar–CNTs catalyst could be promising electrocatalyst for PEMFCs with high utilization and durability.

Acknowledgment

This work was financially supported by the China National 973 Program (2012CB215500 and 2012CB720300), by the NSFC of China (Grant Nos. 21176327 and 21276291), and by the Fundamental Research Funds for the Central Universities (CDJZR12228802).

References

[1] H.W. Zhang, P.K. Shen, Chem. Rev. 112 (2012) 2780–2832.
[2] Z.G. Qi, A. Kaufman, J. Power Sources 114 (2003) 21–31.
[3] K.M. Yeo, S. Choi, R.M. Anisur, J. Kim, I.S. Lee, Angew. Chem. Int. Ed. 50 (2011) 745–748.
[4] B. Lim, M.J. Jiang, P.H.C. Camargo, E.C. Cho, J. Tao, X.M. Lu, Y.M. Zhu, Y.N. Xia, Science 324 (2009) 1302–1305.
[5] S.Y. Wang, L.P. Zhang, Z.H. Xia, A. Roy, D.W. Chang, J.B. Baek, L.M. Dai, Angew. Chem. Int. Ed. 51 (2012) 4209–4212.
[6] J. Liang, Y. Jiao, M. Jaroniec, S.Z. Qiao, Angew. Chem. Int. Ed. 51 (2012) 11496–11500.
[7] H. Tsuchiya, O. Kobayashi, Int. J. Hydrogen Energy 29 (2004) 985–990.
[8] D. Lee, S. Hwang, Int. J. Hydrogen Energy 33 (2008) 2790–2794.
[9] E. Passalacqua, F. Lufrano, G. Squadrito, A. Patti, L. Giorgi, Electrochim. Acta 46 (2001) 799–805.
[10] G. Sasikumar, J.W. Ihm, H. Ryu, J. Power Sources 132 (2004) 11–17.
[11] A. Ferrandez, S. Baranton, J. Bigarre, P. Buvat, C. Coutanceau, Langmuir 28 (2012) 17832–17840.
[12] P. Gode, F. Jaouen, G. Lindbergh, A. Lundblad, G. Sundholm, Electrochim. Acta 48 (2003) 4175–4187.
[13] Z.Q. Xu, Z.Q. Qi, A. Kaufman, Electrochem. Solid-state Lett. 69 (2003) A171–A173.
[14] S. Zhu, S.L. Wang, L.H. Jiang, Z.X. Xia, H. Sun, G.Q. Sun, Int. J. Hydrogen Energy 37 (2012) 14543–14548.
[15] J.M. Song, S. Suzuki, H. Uchida, M. Watanabe, Langmuir 22 (2006) 6422–6428.
[16] S.G. Chen, Z.D. Wei, H. Li, L. Li, Chem. Commun. 46 (2010) 8782–8784.
[17] C.A. Dyke, J.M. Tour, J. Am. Chem. Soc. 125 (2003) 1156–1157.
[18] T.J. Schmidt, H.A. Gasteiger, G.D. Stab, P.M. Urban, D.M. Kolb, R.J. Behm, J. Electrochem. Soc. 145 (1998) 2354–2358.
[19] S. Sun, G. Zhang, D. Geng, Y. Chen, R. Li, M. Cai, X. Sun, Angew. Chem. 123 (2011) 442–446.
[20] J.C. Yang, M.J. Jablonsky, J.W. Mays, Polymer 43 (2002) 5125–5132.
[21] Z.P. Sun, X.G. Zhang, R.L. Liu, Y.Y. Liang, H.L. Li, J. Power Sources 185 (2008) 801–806.
[22] H.S. Oh, K. Kim, Y.J. Ko, H. Kim, Int. J. Hydrogen Energy 35 (2010) 701–708.
[23] S.G. Chen, Z.D. Wei, L. Guo, W. Ding, L.C. Dong, P.K. Shen, X.Q. Qi, L. Li, Chem. Commun. 47 (2011) 10984–10986.